Journal of Nonlinear and Convex Analysis
Volume 26, Number 7, 2025, 2015–2026

Yokohama Publishers
ISSN 1880-5221 ONLINE JOURNAL

YOLCD: A DEFECTS DETECTION METHOD FOR CIGARETTE PACKAGING BASED ON CLO ATTENTION AND CONTEXT AUGMENTATION

HAIFENG SONG AND SHENGHAI KE*

Abstract. Detecting defects is vital for cigarette product quality checks. This paper presents YOLCD, a method for identifying cigarette packaging defects using Clo attention and context augmentation. Firstly, We achieved a comprehensive and detailed analysis of cigarette image features by integrating the Clo attention mechanism into the Backbone of YOLOv8. This mechanism combines global and local perspectives, reshaping the Bottleneck structure and enhancing the model's feature capture. Secondly, to improve small target detection and inter-layer semantic information transfer, we embedded the CAM module before the 20th layer of the Neck module. This addresses the dispersion of small target features and enhances YOLOv8's detection precision and robustness. Finally, we propose the ECIoU loss function, which builds on the CIoU function by considering bounding box center offset, aspect ratio changes, and shape differences, thus refining the model's optimization. Experimental results indicate that YOLCD excels with a precision of 91.81%, mAP of 91.67%, and recall of 91.56%, confirming its utility in cigarette packaging defect detection.

1. Introduction

China is the world's largest producer and consumer of tobacco. In 2021, it achieved a record tax revenue of 1,358.1 billion yuan, contributing 1.187% to GDP [3]. However, production issues such as machine errors can cause defects like creases, distortion, punctures, and stains, impacting aesthetics, taste, and quality [26]. These defects can lead to financial and reputational damage, highlighting the need for rapid and precise defect detection to ensure product quality.

Cigarette packaging defect detection involves machine vision and deep learning technologies. Machine vision simulates human vision for real-time monitoring, involving image acquisition, preprocessing, feature extraction, and classification [8, 14]. The approach utilizes techniques such as SVM [22] and incorporates systems like Linear and Cross Detection Platforms [5]. However, it exhibits sensitivity to variations in lighting and environmental conditions. Deep learning models

2020 *Mathematics Subject Classification.* 62H35, 68T10.

Key words and phrases. Cigarette packaging, defects detection, Clo attention, CAM, ECIoU.

This research was supported by the national social science foundation art general project of China (23BG123), the national natural science foundation project of China (62473004), Zhejiang provincial department of science and technology soft science research program (2025C35056), the science and technology planning projects of Taizhou (24nya03), the education and science planning project of Taizhou (TG24032), the general scientific research projects of Zhejiang provincial department of education (Y202249832), the innovation and entrepreneurship training program (2024103500046), Zhejiang provincial educational science planning project (2025SCG159).

*Corresponding author.

like AlexNet [7], GoogLeNet [20], VGG16 [18], and ResNet [4] have been applied to detection tasks but struggle with cigarette defect features. YOLO and its variants are widely used for defect detection, including cigarette packaging, offering automatic feature extraction and high accuracy [2,19]. However, challenges remain: (1) models are not optimized for cigarette defects, limiting feature extraction; (2) small object detection issues are not fully resolved; (3) YOLO's loss function lacks consideration for bounding box shape variations, impacting the detection of diverse defect shapes.

To address these issues, we propose You Only Look at Cigarette Defects (YOLCD), a method leveraging Clo attention and context augmentation for cigarette packaging defect detection. Key contributions include: (1) YOLCD enhances feature extraction for cigarette defect detection with Clo attention, merging global and local views to refine the Bottleneck structure and improve complex feature analysis. (2) YOLCD incorporates a Context-Augmented Module (CAM) before the 20th Neck layer to boost small object detection, addressing scattered feature and semantic information disparities. (3) YOLCD addresses YOLOv8's loss function limitations with an Enhanced CIoU (ECIoU) loss, accounting for center distance, aspect ratio, and shape differences to enhance model optimization.

2. Related works

2.1. **Research on defect detection based on deep learning.** Recent advances in deep learning have driven the evolution of object detection. Li [9] proposed a lightweight Faster R-CNN algorithm for cigarette packaging defect detection, achieving 97.34% accuracy. Liu Yajiao's Steel-YOLOv3 model achieves an accuracy of 89.24% in detecting surface defects on steel materials [12]. Rizwan [17] introduced a two-stage CNN for anomaly segmentation, improving AP by 6.2%. Liu [11] developed LF-YOLO for X-ray weld defect detection, achieving 92.9% mAP and 61.5 FPS. FE-YOLO model which is designed for industrial surface defect detection, utilizes depthwise separable convolutions and advanced feature pyramid networks to enhance both detection accuracy and speed [24].

The aforementioned research employed deep learning-based object detection algorithms to identify defects in various products. Each algorithm was customized for specific defect types, improving performance over original versions. However, these adaptations were dataset-specific and overlooked the unique features of cigarette defects. As a result, the proposed models are unsuitable for cigarette defect detection, necessitating further in-depth research tailored to this domain.

2.2. **Research on the cigarette defect detection.** Research shows limited use of deep learning-based object detection for cigarette defects. Jia W [6] compared YOLOv3 and Faster R-CNN for cigarette carton defects, proposing solutions for size and position measurement, while YOLOv5 is used for real-time packaging inspection. Park H M [15] optimized YOLOv4-Tiny for cigarette detection. To address minor defect identification, Zhu [27] developed CDD-YOLOv8 with a small object detection component and CBAM for improved small defect detection. Liu

Hongyu [10] enhanced YOLOv5s with SE-Net, Leaky ReLU, and DIoU Loss, boosting mAP by 3.3-3.8% and achieving 4.7ms detection speed for real-time factory applications.

Similar to prior research, this study is based on the YOLOv8 model while introducing several distinctive enhancements: (1) Taking into account attribute features and scale differences, it provides a comprehensive classification of cigarette defects into seven types, presenting a formidable challenge for detection algorithms. (2) The backbone network is augmented with a Contextual Attention Module (CAM), enabling the model to effectively capture both global and local features. (3) The implementation of the EIoU loss function optimizes the model's capability to detect defects across diverse sizes and shapes, resulting in improved detection accuracy and better alignment with industrial requirements.

3. Proposed methods

3.1. **YOLOv8.** YOLOv8 is a deep learning-driven object detection algorithm. It comprises four parts: the input layer, the backbone network, the feature fusion layer, and the detection head. The network architecture of YOLOv8 is shown in Figure 1:

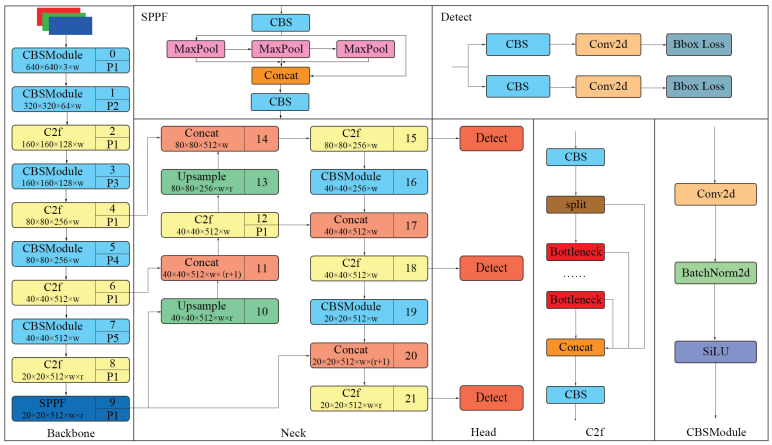

Figure 1. The network architecture of YOLOv8.

3.2. **Improvement of backbone.** To enhance YOLOv8's Backbone for cigarette defect extraction, the C2f model was improved by integrating the Clo attention mechanism and reconstructing the Bottleneck. As shown in Figure 2, a dual-branch Clo block (Global and Local) was added after convolution in the Bottleneck. The Local branch employs depthwise separable convolutions to capture high-frequency information, enhancing local features, while the Global branch extracts low-frequency global information through linear transformations to obtain Q_{global}, K_{globla} and V_{globla}, followed by downsampling and standard attention operations (Equations (3.1) and (3.2)).

$$Q_{global}, K_{global}, V_{global} = FC(X_{in}), \tag{3.1}$$

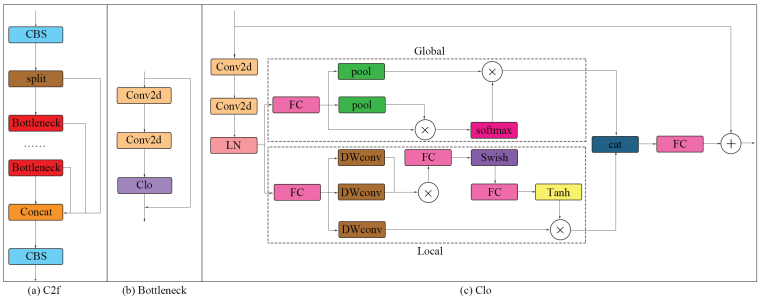

FIGURE 2. The architecture of C2f, Bottleneck and Clo.

$$X_{global} = Attn(Q_{global}, Pool(K_{global}), Pool(V_{global})). \tag{3.2}$$

X_{in} is the input of the global branch, FC is the fully connected layer. Similar to the global branch, the Local branch first obtains the local Q_{global}, K_{globla} and V_{globla} through a linear transformation. For V_{globla}, local information aggregation is performed using depthwise separable convolution (DWconv), as shown in Equations (3.3) and (3.4):

$$Q_{local}, K_{local}, V_{local} = FC(X_{in}), \tag{3.3}$$

$$V_{DW} = DWconv(V_{local}). \tag{3.4}$$

The weights of $DWconv$ are globally shared. After integrating the local information of V_{local} using shared weights, Q_{local} and K_{local} are combined to generate contextually aware weights. Specifically, two $DWconvs$ are used to aggregate Q_{local} and K_{local} separately. Then, to obtain contextually aware weights ranging between -1 and 1, the Hadamard product of Q_{local} and K_{local} is calculated. Finally, the obtained weights are used to enhance local feature information with contextual awareness. As shown in Equations (3.5) to (3.8):

$$Q_L = Dwconv(Q_{local}), K_L = DWconv(K_{local}), \tag{3.5}$$

$$Attn_t = FC(Swich(FC(Q_L \odot K_L))), \tag{3.6}$$

$$Attn = tanh\Big(\frac{\sqrt{d}}{Attn_t}\Big), \tag{3.7}$$

$$X_Local = Attn \odot V_{DW}. \tag{3.8}$$

d is the number of channels, $\odot$ is the Hadamard product. Finally, the outputs of the two branches are concatenated and a fully connected layer is calculated to obtain the final output, as shown in Equation (3.9):

$$X_{out} = Concat(FC(X_{local}, X_{Global})). \tag{3.9}$$

3.3. **Improvement of the neck.** Cigarette packaging defects typically occupy a minimal portion of the overall image, making damage detection a small target detection problem. To address dispersed small target features and semantic discrepancies between layers, a Context Augmentation Module (CAM) is added before the SPPF output and the 20th layer of the Neck module. The CAM architecture is illustrated in Figure 3.

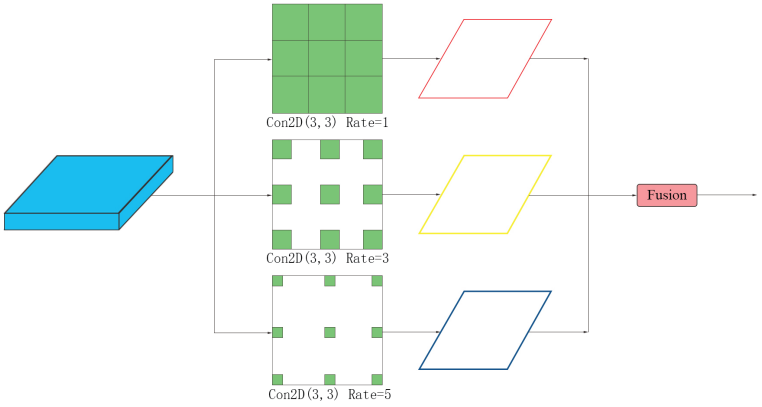

FIGURE 3. The architecture of CAM.

As can be seen from Figure 4, with the same 3×3 convolution, it can achieve the effect of 5×5 or 7×7 convolution. Assuming the dilation rate is d, the dilated convolution's kernel size is K, and the stride of the ith layer is $Stride_i$, the formula for calculating the equivalent kernel size K' is shown in Equation (3.10):

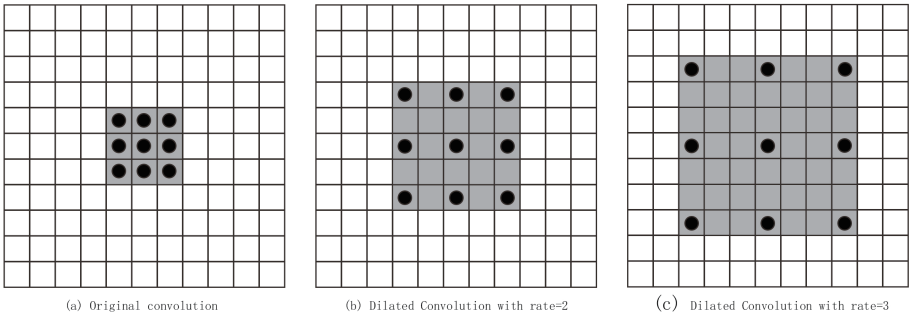

FIGURE 4. The dilation rate of dilated convolution.

$$k^{'} = k + (k-1) \times (d-1). \tag{3.10}$$

R_{i+1} is the current layer's receptive field, R_i is the previous layer's receptive field, and $k^{'}$ is the size of the convolution kernel, then Equation (3.11) can be expressed as:

$$R_{i+1} = (k^{'} - 1) \times S_i + R_i. \tag{3.11}$$

Where S_i represents the product of the strides of all previous layers, which can be calculated by Equation (3.12):

$$S_i = \prod_{i=0}^{n} Stride_i. \tag{3.12}$$

To ensure a global scan of the cigarette packaging feature map, we use three 3×3 convolutional kernels with dilation rates of 1, 3, and 5 to extract multi-scale features. The feature extraction results are then combined through fusion strategies with addition, concatenation, and adaptation.

3.4. **Improvement of loss.** YOLOv8 uses CIoU as its loss function, which considers overlap and size differences but ignores bounding box shape differences. Since defective cigarette packaging shapes vary significantly across categories, scale variations can reduce detection accuracy. To address this, we propose an enhanced loss function, ECIoU, which incorporates center distance, aspect ratio, and shape differences (Equation (3.13)).

$$ECIou = 1 - IoU + \alpha v + \frac{\rho^2(b^{gt}, b)}{c^2} + \frac{\rho^2(h^{gt}, h)}{c_h^2} + \frac{\rho^2(w^{gt}, w)}{c_w^2}. \tag{3.13}$$

Where IoU is the ratio of the intersection area to the union area. $T^{gt} = (m^{gt}, n^{gt}, k^{gt}, g^{gt})$ is the truth bounding box, $P = (m, n, k, g)$ is the predicted bounding box, m, n is the center point of the bounding box, w, h is the width and heigh. b and b_{gt} the center of the predicted bounding box and the truth bounding box. $\rho(\cdot)$ is the Euclidean distance. $\rho^2(b^{gt}, b)$ is the square of the distance between the centers of the predicted bounding box and the truth bounding box. c is the diagonal length of the smallest bounding box that encompasses both boxes. v is the consistency parameter. α a is a balancing parameter that assigns priority based on the IoU value. c_h represents the height ratio. c_w represents the width ratio.

4. Experimental results

4.1. **Dataset and experiment parameters.** The cigarette appearance defect images were collected in a laboratory using a Liangtian S1020A3 camera, adhering to the national GB5606-2005 standards. The setup ensured consistent shooting angles and lighting conditions. Experimental equipment and parameters are detailed in Figure 5.

We categorize cigarette packaging defects into eight types, as shown in Figure 6. We encode the cigarette appearance defects, with specific encoding rules presented in Table 1. A total of 4500 cigarette defect images (Some examples of defects are derived from real-world manufacturing conditions.) were annotated using the LabelImg tool, with annotations stored in XML format. The dataset was split into training, validation, and test sets in a 6:3:1 ratio. Experiments were conducted on a high-performance workstation with an Intel Core i9-11900 CPU (2.50 GHz), 32 GB DDR4 RAM, 1 TB SSD, and an NVIDIA GeForce RTX 3060 GPU (12 GB VRAM). YOLOv8 was optimized using the Adam optimizer with an initial learning rate of 0.001 (exponential decay), momentum of 0.9, and 80 epochs.

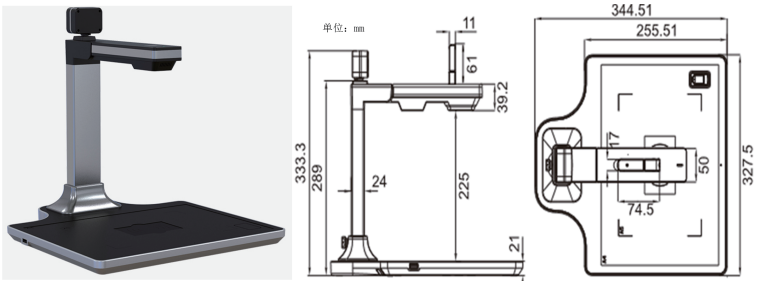

FIGURE 5. The experimental equipment and parameters.

FIGURE 6. The cigarette packaging defects.

We have adopted the following methods to address the challenges posed by variations in lighting, different packaging materials, and printing defects: (1) Data Augmentation for Invariance: We have employed extensive data augmentation techniques to simulate various lighting conditions, including random variations in brightness, contrast, hue, and saturation. By training the model with such a diverse set of images, we have enhanced its ability to generalize across different lighting scenarios. (2) Histogram Equalization: To improve the visibility of objects under varying lighting conditions, we preprocess images using histogram equalization, which helps to normalize the intensity distribution within the images. (3) Robust Feature Extraction: Similar to handling lighting variations, we focus on extracting features that are less affected by printing defects, such as the overall shape and structural patterns of the packaging.

4.2. **Evaluation methods.** In the experiment, the evaluation indicators used include accuracy (P), recall rate (R), average accuracy (mAP), frames per second

TABLE 1. Cigarette appearance defects encoding

Num.	Encoding	Defects name	Defects description
1	00ZC	Normal	Normal cigarette, no abnormality
2	01CP	Puncture	Common in the paper loading part
3	02WD	Stain	It's on both cigarette paper and mounting paper
4	03BK	Crevasse	It is common in the smoke stem and the defective area is large
5	04CY	misaligned	The position of the paper at the connection between the cigarette paper and the loading paper is incorrect.
6	05ZZ	Wrinkle	Common cigarette appearance defects, cigarette paper and mounting paper have this defect
7	06QB	Warped	Only the defects at the loading of the paper are considered
8	07NQ	Distortion	Mainly in the smoke rod part, the defects are more obvious
9	08JM	Entrained	Pack tobacco at the package junction

processed (FPS) and F1-score ($F1$) which are used to measure the performance and effectiveness of the YOLCD.

4.3. **Experiment results and comparison.**

4.3.1. *Ablation experiment.* To validate the effectiveness of each proposed improvement strategy, ablation experiments were conducted on our self-built cigarette packaging defects dataset. Results are shown in Table 2, where (✓) and (×) denote the use or absence of the corresponding optimization method, respectively.

TABLE 2. Ablation experiment results.

Model	Backbone	Neck	ECIoU	P	R	mAP
YOLOv8	×	×	×	88.31	89.07	88.47
	✓	×	×	88.21	89.64	88.98
	×	✓	×	88.86	88.93	88.75
	×	×	✓	90.18	89.94	90.20
	✓	✓	×	90.89	91.22	90.84
	×	✓	✓	90.68	90.97	90.72
	✓	×	✓	91.72	91.48	91.52
	✓	✓	✓	91.81	91.56	91.67

The experimental results in Table 1 show that each improvement strategy enhances the baseline model's detection performance. Integrating the Clo attention mechanism into the Backbone and replacing the C2f module with a dual-branch attention mechanism in the Bottleneck improves feature extraction, increasing mAP by 0.51%. Adding the Context-Augmented CAM module in the Neck addresses

small target feature dispersion and semantic differences, boosting mAP by 0.32%. Replacing the bounding box regression loss with ECIoU introduces a shape difference penalty, improving object localization accuracy for diverse cigarette packaging defects and increasing mAP by 1.73%.

4.3.2. *Loss function comparison.* To verify the superiority of ECIoU, we conducted comparative experiments on the YOLOv8 model using ECIoU and some mainstream loss functions, while keeping other training conditions consistent. The experimental results are shown in Table 3 and Figure 7a. The results indicate that when ECIoU is used as the bounding box regression loss, the model achieves the best detection performance. Moreover, the mAP of the model using ECIoU is 3.5% higher than that using CIoU, which demonstrates the effectiveness of ECIoU.

TABLE 3. The contrast experiment results of the loss function.

Loss function	**P**	**R**	**mAP**
CIoU	88.25	88.47	88.17
DIoU	89.63	89.39	89.48
GIoU	90.27	90.53	90.39
EIoU	90.84	90.67	90.41
SIoU	91.33	91.24	91.19
ECIoU	91.81	91.56	91.67

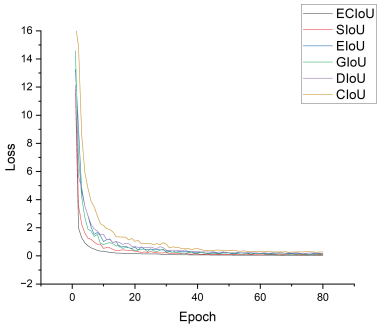

(A) Comparison of loss function.

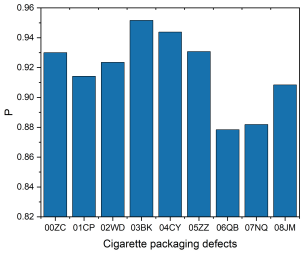

(B) The experiment result of YOLCD.

FIGURE 7. Experiment results of different loss function and YOLCD

4.3.3. *Different method comparison.* To further validate the advancement of the YOLCD, we conducted comparative experiments with current classic object detection algorithms on the same experimental equipment and dataset. The selected object detection algorithms include Faster RCNN [9], YOLOv5 [16], CJS-YOLOv5n [13], Enhanced SSD [23], YOLOv6 [1], YOLOv7 [21], and YOLOv8 [25].

The experiments results of the YOLCD are shown in Figure 7b, As can be seen from Figure 7b, an accuracy of more than 87% has been achieved in all nine categories of cigarette packaging defects. Among them, defects 06QB and 07NQ have

the lowest detection accuracy due to their inconspicuous image features. Defects 03BK and 04CY have the highest detection accuracy because their image features are significantly different. In all, a detection accuracy of 91.81% has been achieved in all categories.

Table 4. Comparative experimental results.

Model	**P**	**R**	**mAP**	**FPS**	**F1**
Faster RCNN	75.84	72.96	76.47	18	74.32
YOLOv5	84.35	83.37	83.89	126	84.17
CJS-YOLOv5n	85.92	86.18	85.81	142	85.22
Enhanced SSD	86.17	86.34	85.58	52	85.49
YOLOv6	86.59	85.84	86.33	154	85.92
YOLOv7	87.19	87.92	87.38	178	87.56
YOLOv8	88.31	89.07	88.47	193	89.19
YOLCD	91.81	91.56	91.67	211	91.72

The results of the comparative experiments are shown in Table 4. As shown in Table 4, firstly, compared with YOLOv6 and YOLOv7, our improved model not only achieved an increase of 4.29% and 5.34% in mAP respectively, but also significantly improved in FPS and F1 score. Secondly, in comparative experiments with several currently popular object detection models, our improved model ensured faster detection speed while enhancing mAP, with the detection speed being four times that of Enhanced SSD. Finally, based on the comparative experimental results of this study, the YOLCD model outperformed the original YOLOv8 model and other mainstream object detection algorithms in terms of accuracy, recall rate, F1 score, and detection speed, confirming the advantages of the proposed improvement methods.

5. Conclusions

To address the low accuracy, poor real-time performance, and environmental impact of current cigarette packaging defect detection algorithms, this study proposes the YOLCD algorithm. By analyzing YOLOv8's limitations in practical detection, the model was improved in three key areas: (1) Enhancing the Backbone's C2f module with a Clo attention mechanism (Global and Local branches) and reconstructing the Bottleneck structure to boost feature extraction for cigarette packaging defects; (2) Adding a context augmentation module before the 20th layer of the Neck to address scattered small target features and semantic differences, improving small target recognition; and (3) Introducing the ECIoU loss function, which considers center distance, aspect ratio, and shape differences, enhancing model optimization. Experimental results show improved accuracy and model stability while retaining YOLOv8's compact size and fast detection. Future work will explore model compression techniques, such as pruning and quantization, to further reduce model size and enhance efficiency.

References

[1] N. Barazida, *YOLOv6: A Single-Stage Object Detection Framework for Industrial Applications*, arXiv: 2209.02976v1, (2024), 1–17.

[2] B. N. Chen, Z. Y. Wang, R. Xia, and M. Chen, *Text image recognition algorithm of Qin bamboo slips based on lightweight AlexNet network*, Journal of Central South University (Science and Technology) **54** (2023), 3506–3517.

[3] China Tobacco Network, *RMB 1.3581 trillion and RMB 1.2442 trillion! China's tobacco industry's tax revenue and fiscal revenue reached a record high*, China Tobacco Network, (2022), https://nx.tobacco.gov.cn/5/4469.html.

[4] K. He, X. Zhang, S. Ren and J. Sun, *Deep residual learning for image recognition*, in: Proceeding of The IEEE Computer Society Conference on Computer Vision and Pattern Recognition, IEEE, 2016, pp. 770–778.

[5] C. Huang, H. Lu, X. Huang, S. Chen and M. Chen, *Research on defect detection algorithm for cigarette case appearance based on machine vision*, in: Proceeding of The 2022 International Conference on Wireless Communications, Networking and Applications, Springer, 2023, pp. 287–296.

[6] W. P. Jia, W. Chu, W. T. Liu, K. Huang, C. Q. Li and F. Wu, *Surface defect detection method for corrugated box for cigarettes based on YOLO v3 algorithm*, China Pulp and Paper, **42** (2023), 126–133.

[7] A.Krizhevsky, A. Sutskever and G. E. Hinton, *ImageNet classification with deep convolutional neural networks*, Communications of the ACM **60** (2017), 84–90.

[8] J. Li, H. H. Lu, X. Wang, J. H. Hong, S. Wang, L. X. Shen, J. Bao and G. H. Xiao, *Online cigarette appearance inspection system based on machine vision*, Tobacco Science and Technology **52** (2019), 109–114.

[9] L. F. Li, M. D. Li and H. Z. Hu, *An algorithm for cigarette capsules defect detection based on lightweight faster RCNN*, in: Proceeding of The Chinese Control Conference, CCC, 2021, pp. 8028–8034.

[10] H. Y. Liu and G. W. Yuan, *Detection of cigarette appearance defects based on improved YOLOv5s*, Computer Technology and Development **32** (2022), 161–167.

[11] M. Y. Liu, Y. P. Chen, J. M. Xie, L. He and Y. Zhang. *LF-YOLO: A lighter and faster YOLO for weld defect detection of X-ray image*, IEEE Sensors Journal **23** (2023), 7430–7439.

[12] Y. J. Liu, H. T. Yu, J. Wang, L. F. Yu and C. H. Zhang, *Surface detection algorithm of multi-shape small defects for section steel based on deep learning*, Journal of Computer Applications **42** (2022), 2601–2608.

[13] Y. H. Ma, G. W. Yuan, K. Yue and H. Zhou, *CJS-YOLOv5n: A high-performance detection model for cigarette appearance defects*, Mathematical Biosciences and Engineering **20** (2023), 17886–17904.

[14] D. Murthy, R. R. Ouellette, T. Anand, S. Radhakrishnan, N. C. Mohan, J. Lee and G. Kong, *Using computer vision to detect E-cigarette content in TikTok videos*, Nicotine and Tobacco Research **26** (2024), 36–42.

[15] H. M. Park and J. H. Park, *YOLO Network optimization with a single circular bounding box for detecting defective cigarettes*, IEEE Access **11** (2023), 142951–142963.

[16] Y. Peng, D. Jiang, X. Z. Lv and Y. B. Liu, *Efficient and high-performance cigarette appearance detection based on YOLOv5*, in: Proceeding of the International Conference on Intelligent Perception and Computer Vision, IEEE, 2023, pp 7–12.

[17] R. A. Shah, O. Urmonov and H. W. Kim, *Two-stage coarse-to-fine image anomaly segmentation and detection model*, Image and Vision Computing, **139** (2023): 104817.

[18] K. Simonyan and A. Zisserman, *Very deep convolutional networks for large-scale image recognition*, in: Proceeding of The 3rd International Conference on Learning Representations, ICLR, 2015, pp. 1–12.

[19] K. K. Sudha and P. Sujatha, *A qualitative analysis of googlenet and alexnet for fabric defect detection*, International Journal of Recent Technology and Engineering **8** (2019), 86–92.

[20] C. Szegedy, W. Liu, Y. G. Jia, P. Sermanet, S. Reed, D. Anguelov, D. Erhan, V. Vanhoucke and A. Rabinovich, *Going deeper with convolutions*, in: Proceeding of The IEEE Computer Society Conference on Computer Vision and Pattern Recognition, IEEE, 2015, pp. 1–9.
[21] C. Y. Wang, A. Bochkovskiy and H. Liao, *Yolov7: Trainable bag-of-freebies sets new state-of-the-art for real-time object detectors*, in: Proceeding of The IEEE Conference on Computer Vision and Pattern Recognition (CVPR), IEEE, 2023, pp 7464–7475.
[22] Q. F. Wen and X. F. Ji, *Cigarette box code recognition based on machine vision*, Frontiers in Computing and Intelligent Systems **1** (2022), 38–40.
[23] S. C. Wu, X. Z. Lv, Y. B. Liu, M. Jiang, X. X. Li, D. Jiang, J. Yu, Y. Y. Gong and R. Jiang, *Enhanced SSD framework for detecting defects in cigarette appearance using variational Bayesian inference under limited sample conditions*, Mathematical Biosciences and Engineering **21** (2024), 3281–3303.
[24] Y. F. Xie, W. T. Hu, S. W. Xie and L. He. *Surface defect detection algorithm based on feature-enhanced YOLO*, Cognitive Computation **15** (2023), 565–579.
[25] M. Yaseen, *What is YOLOV8: An in-depth exploration of the internal features of the next-genertion objcet detetor*, arXiv: 2408.15857V1, (2024), 1–10.
[26] G. W. Yuan, J. C. Liu, H. y. Liu, Y. H. Ma, H. Wu and H. Zhou, *Detection of cigarette appearance defects based on improved YOLOv4*, Electronic Research Archive **31** (2023), 1344–1364, .
[27] L. M. Zhu, J. Zhang, Q. Zhang and H.T. Hu, *CDD-YOLOv8: A small defect detection and classification algorithm for cigarette packages*, in: Proceeding of 13th IEEE International Conference on CYBER Technology in Automation, Control, and Intelligent Systems, CYBER, 2023, pp: 716–721.

Manuscript received October 24, 2024
revised February 26, 2025

Haifeng Song
School of Art and Design, Taizhou University, Taizhou 318000, Zhejiang, China
E-mail address: isshf@tzc.edu.cn

Shenghai Ke
School of Art and Design, Taizhou University, Taizhou 318000, Zhejiang, China
E-mail address: ksh@tzc.edu.cn